

Eigenbackground Revisited: Can We Model the Background with Eigenvectors?

Mahmood Amintoosi^{*1} and Farzam Farbiz²

¹Faculty of Mathematics and Computer Science, Hakim Sabzevari University, Iran

²A*STAR Institute of High Performance Computing (IHPC), 1 Fusionopolis Way, #16-16 Connexis, Singapore 138632

Abstract—Using dominant eigenvectors for background modeling (usually known as Eigenbackground) is a common technique in the literature. However, its results suffer from noticeable artifacts. Thus have been many attempts to reduce the artifacts by making some improvements/enhancement in the Eigenbackground algorithm.

In this paper, we show the main problem of the Eigenbackground is in its own core and in fact, it is not a good idea to use strongest eigenvectors for modeling the background. Instead, we propose an alternative solution by exploiting the weakest eigenvectors (which are usually thrown away and treated as garbage data) for background modeling. MATLAB codes are available at <https://github.com/mamintoosi/Eigenbackground-Revisited>.

Keywords— Eigenbackground, Background Modeling, Background Subtraction, Principal Component Analysis, Gaussian Mixture Model, Video Analysis.

I. INTRODUCTION

Background segmentation is one of the fundamental tasks in computer vision with a wide spectrum of applications from video compression to scene understanding. A very commonly used example of background segmentation is on detecting moving objects in videos taken from static cameras, by finding the differences between the new frame and the background model of the scene (or the reference frame).

There have been several background subtraction and modeling methods in the literature. All of these methods aim to effectively estimate the background model from a temporal sequence of a video frames. One of a well-known method in this field is Eigenbackground method [1] that models the background by a set of dominant eigenvectors. The idea has been used in many papers including [2]–[24] for background segmentation. In some literature, this method has been also called as PCA and Subspace Learning.

According to [1] the core idea of Eigenbackground method is as follow:

“In order to reduce the dimensionality of the space, in principal component analysis (PCA) only M eigenvectors (eigenbackgrounds) are kept, corresponding to the M largest eigenvalues to give a Φ_M matrix.”

The advantage of this method is that it is a mathematically straightforward algorithm, which requires no heuristics or parameters that must be set manually. However, most of research



Fig. 1. The result of the PCA model (Fig. 8 of [19]) in background modelling. From top to bottom, the original images, ground truth and the results of PCA (courtesy from [19]).

articles that used this method highlighted its rather poor quality result in background modeling especially in the presence of some foreground objects in the input video frames. Please see figures 1 and 2. as an example of the Eigenbackground’s performance in modeling the background.

In [1] it is claimed that the eigenspace provides a model for the background:

“...the eigenspace provides a robust model of the probability distribution function of the background, but not for the moving objects”

In contrast to this statement, in this paper we will show that the eigenspace is indeed influenced by moving objects, not by the static parts of the scene. This is actually the same as the concept of eigenfaces, which models the faces and not the background. In our previous papers [25], [26] we demonstrated the efficiency of the usage of eigenvectors related to weak eigenvalues, by QR factorization; here our claim is extended and mathematically proved.

The rest of this paper is organized as follows. In Section II we review the Eigenbackground algorithm and we show why it fails to properly model the background images by an example. Section III devotes to the theoretical aspects of the problem. Further examples and experiments are demonstrated in Section IV. The conclusions are provided in Section V. Finally, we explain some of the lemmas used in the paper in Appendix as a separate file.

In summary, the contributions of this paper are as follows:

- 1) To prove why Eigenbackground algorithm is not suitable for background modeling
- 2) To propose an alternative to Eigenbackground, by using the weakest eigenvectors (which are usually treated



(a) Original input images for learning

(b) Learned *polluted* background due to foreground objects

Fig. 2. The poor quality of the learned background model due to foreground objects (Fig. 4 of [7], courtesy from [7]).

thrown away in the processing and are treated as garbage data) for modeling the background of a video frame.

II. REVIEW OF EIGENBACKGROUND ALGORITHM

Eigenbackgrounds represent the background as a set of dominant eigenvectors, extracted from a set of training images. As mentioned in [1]:

“Note that moving objects, because they don’t appear in the same location in the N sample images and they are typically small, do not have a significant contribution to this model. Consequently, the portions of an image containing a moving object cannot be well-described by this eigenspace model (except in very unusual cases), whereas the static portions of the image can be accurately described as a sum of the various eigenbasis vectors. That is, the eigenspace provides a robust model of the probability distribution function of the background, but not for the moving objects.”

The dominant eigenvectors are then used to estimate static parts of the scene to form the background image in this method.

However, there has been no proof for the above assumption. Although the moving objects might cover only small parts from the video frames, but it does not mean they will not affect the dominant eigenvectors in a significant way.

To test the above assumption, which is indeed the core of the Eigenbackground algorithm, let’s review the eigenvectors in a matrix. For this review, we use the concept of principle component analysis (PCA) as its values are calculated using eigenvectors.

It is well-known that the first principal component has the largest possible variance (that is, accounts for as much of the variability in the data as possible), and each succeeding component in turn has the highest variance possible under the constraint that it is orthogonal to the preceding components. Knowing PCA components are calculated using eigenvectors of the matrix, the most dominant eigenvector should also be

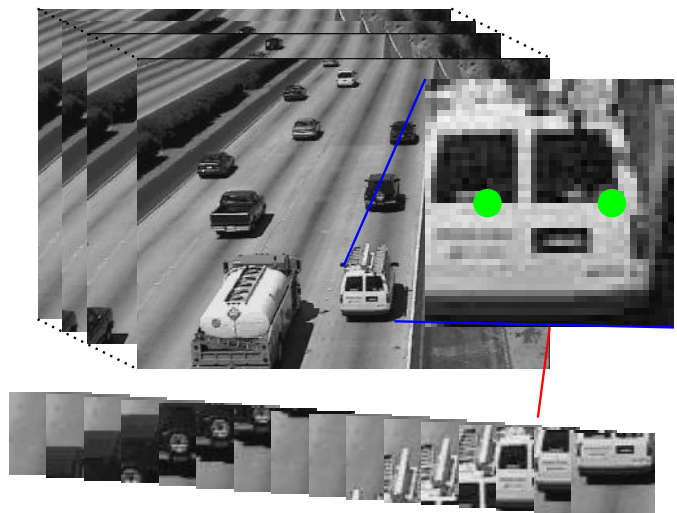


Fig. 3. Sample frames from a highway video scene and the selected block and pixels for Eigenvector analysis.

in the direction with the largest possible variance. In our case study of video frame data, the background images in a video data have little differences from each other and hence their variance is expected to be low. However, a frame with some foreground objects (even if the objects are small), will change the overall variance and therefore it will contribute to the first principle component. This means the strongest eigenvector is indeed affected by any foreground object in video frames.

As can be seen in Figure 1, Eigenbackground method is not able to model background properly due to the presence of foreground objects in the video frames. As another example, readers can see Figure 2 that shows the poor quality of the learned background model due to foreground objects [7]. As mentioned in [10], “It is imperative the background images in the training set do not contain any foreground objects, since they would cause significant errors in the reconstructed background”. Some other works such as [2], [9] tried to use different variations of PCA, including Robust PCA, to improve the performance of Eigenbackground in background subtraction. However, if the training set does not include any foreground objects as suggested in [7], then there is no need to use PCA or Eigenbackground algorithm to model the background and a simple averaging of frame data would provide the background model with less processing time needed. In fact, some papers uses the idea of combining mean image and the first significant eigenvectors of PCA for background modelling (see [16] and [20]).

Let’s analyze the eigenvectors for a test video. Figure 3 shows a sample highway video with 121 frames. We took a 40×40 block of this video and calculated the first three dominant eigenvectors as shown in Figure 4. As can be seen, the dominant PCA are far from the mean value and the background image of this block, and as expected, these PCAs are mostly influenced by foreground objects in the scene.

To further analyze how foreground and background objects affect the eigenvectors, we took the two green pixels from this block so we can display every frame for these two pixels in

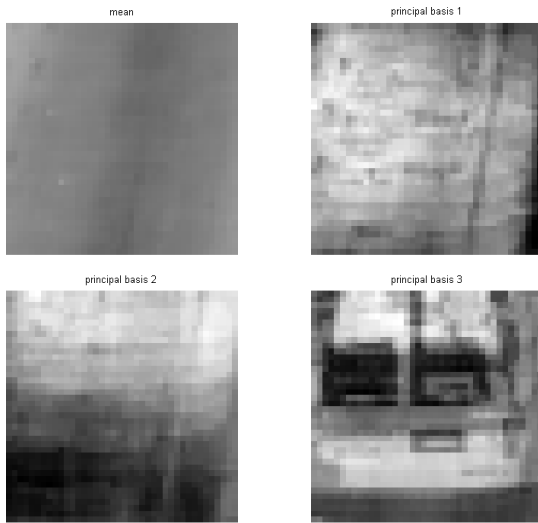


Fig. 4. Mean and 3 first eigenvectors reshaped as the images.

a 2D plot as shown in Figure 5. In this figure, blue crosses are for background frames (92 frames from total 121 frames) and red circles are for foreground frames (29 frames)¹. There are four plots in this figure that shows how the green-line representing the most dominant eigenvector is changed based on the foreground data to the direction that has the maximum variance. As can be seen, almost all background instances are located in one point. The first principal component is influenced mostly by foreground instances. This would be mathematically explained on the following sections, but before that, some more experimental evidences are demonstrated.

Since main eigenvector tends to be in the direction to that maximizes the variance for input data, and each succeeding component in turn has the highest variance possible under the constraint that it is orthogonal to the preceding components, it would be logical to assume the least significant eigenvectors should be the right candidate to model the background image frames. The background image frames are not exactly equal to each other so when we put all frames in one $m \times n$ matrix ($m \geq n$), the rank of the matrix will be the same as the number of frames. But the differences between background frames are much less than foreground ones, and all background frames can be considered as a noisy version of the background model with some small variances. Similar to the concept of Mixture of Gaussian (MoG)[27], where it is assumed pixels with less variance in video frames are likely belong to background and those with higher variance are likely belong to foreground objects, here we can also consider least significant eigenvectors represent background regions.

If the video frames are columnized, a 40×40 block of 100 frames, reshaped as a 1600×100 matrix. Figure 6(a) shows the first 120 rows of the mentioned matrix, with their original order. Reordering these frames based on the R-values of its QR decomposition, leads to figure 6(b) [25], [26]. The diagonal elements of matrix R are called R-values. As can be seen the background frames are more related to weakest R-

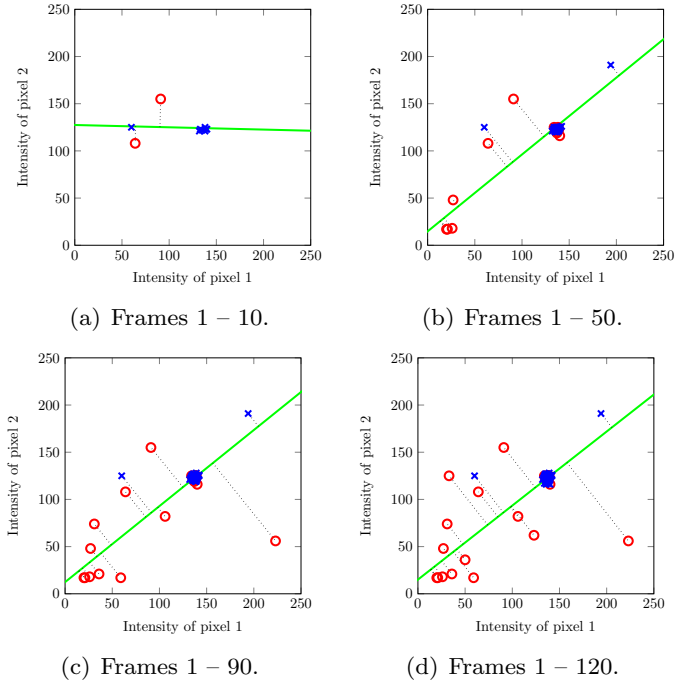


Fig. 5. Change of dominant PCA vector in response to new input frame for two green dotted pixels shown in fig 3. The results are calculated and shown for the first 10, 50, 90, and 120 frames. The background frames are shown by blue x and the foreground frames by red circles. The dominant PCA vector is in the direction that input frames have maximum variance and influenced mostly by foreground frames.

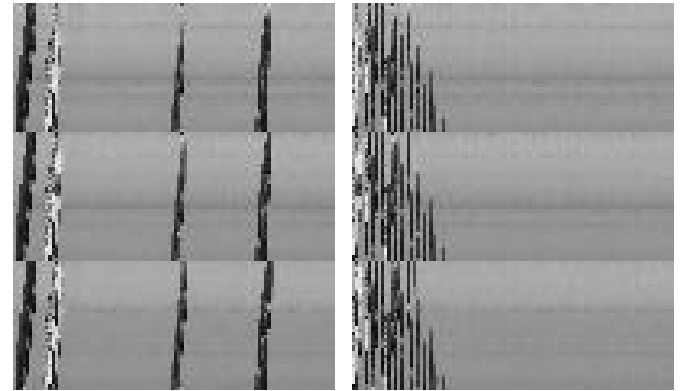


Fig. 6. 100 frames of an instance 40×40 block of *Highway* video shown in the bottom of fig 3: (a) in the temporal order, and (b) in QR decomposition's R-values order. Each frame is columnized. As can be seen the background frames are related to the weakest R-values.

values. R-values are in decreasing order and they tend to track the singular values of P[28]².

To test this idea, we use the *highway* video in Figure 3 and calculated the background using i) 10 most significant and ii) 10 least significant eigenvectors. The results are shown in figures 7 and 8. As expected, the background model is better reconstructed using least significant eigenvectors.

²MATLAB `pca` function can use `svd` and `eig` decomposition methods; The default decomposition method is `svd`.

¹For better demonstration, the frames order is perturbed.

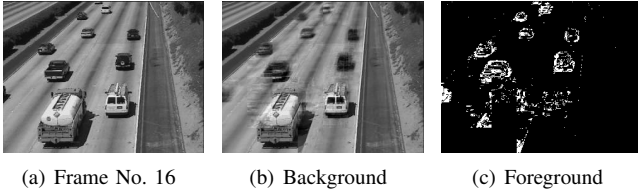


Fig. 7. Background and Foreground models reconstructed using 10 **most** significant eigenvectors.

III. THEORETICAL ASPECTS

In this section we will show that under some assumptions, the foreground instances have the most influence to direction of the strongest eigenvector in PCA. Theoretical results are verified by additional experiments in section IV.

For mathematical discussion some preliminary assumptions and theorems should be explained.

Let $X = \{x_1, \dots, x_n\}$ be the set of n observations with dimensionality D . The goal is to project the data onto a space having dimensionality $M < D$ while maximizing the variance of the projected data. Consider the projection onto a one-dimensional space ($M = 1$). If the direction of this space mentioned by a unit vector e , we shall find vector e such that the projection of $x \in X$ along this direction has maximum variance. each data point x_k is projected onto a scalar value $e^T x_k$. The mean of the projected data is $e^T \mu$, where μ is the sample set mean. The variance of the projected data is given by:

$$\frac{1}{n} \sum_{k=1}^n (e^T x_k - e^T \mu)^2 = \frac{1}{n} e^T S e \quad (1)$$

where S is the scatter matrix:

$$S = \sum_{k=1}^n (x_k - \mu)(x_k - \mu)^T$$

Using Lagrange multipliers method, the eigenvector corresponding to the largest eigenvalue of S , maximizes $e^T S e$.

Our goal is to prove that the eigenvectors corresponding to largest eigenvalues of the scatter matrix S are influenced by foreground frames more than background frames. We will use the assumption in Mixture of Gaussian (MoG) for background modeling of Stauffer and Grimson [27]. In their approach each ‘‘pixel process’’ is a time series of pixel values and these values are modeled by a MoG. In this method it is supposed that:

‘‘... the variance of the moving object is expected to remain larger than a background pixel until the moving object stops.’’

If σ_b, σ_f show the background and foreground variances, respectively, the above assumption means:

$$\sigma_b \ll \sigma_f \quad (2)$$

Suppose that X be intensity values of a particular pixel over times. As a stochastic process, suppose $X = X_b \cup X_f$ is combination of two stochastic process X_b and X_f which

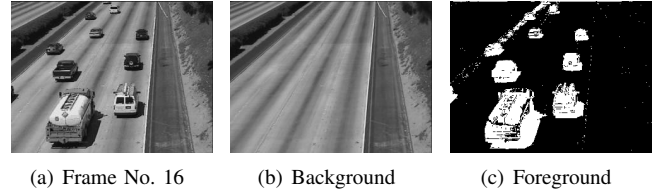


Fig. 8. Background and Foreground models reconstructed using 10 **least** significant eigenvectors.

are those elements belong to background and foreground respectively. From the elementary statistics we have:

$$\mu_{X_b \cup X_f} = \frac{N_b \mu_b + N_f \mu_f}{N_b + N_f} \quad (3)$$

$$\sigma_{X_b \cup X_f}^2 = \frac{N_b \sigma_b^2 + N_f \sigma_f^2}{N_b + N_f} + \frac{N_b N_f}{(N_b + N_f)^2} (\mu_b - \mu_f)^2 \quad (4)$$

where $N_b = |X_b|$ and $N_f = |X_f|$.

Based on assumption (2), since $\sigma_b \ll \sigma_f$ the foreground pixels variance (σ_f^2) has the stronger effect in the total variance.

Let $S_{n-1} = \sum_{k=1}^{n-1} (x_k - m)(x_k - m)^T$ be the scatter matrix, when $X = \{x_1, \dots, x_{n-1}\}$, $x_i \in \mathbb{R}^m$, $i \in \{1, \dots, n-1\}$. We want to show how adding a new instance to X will influence the scatter matrix S . We look for changing the main eigenvector of S , based on the new instance, which may be a background or foreground.

According to Welford algorithm [30], by adding a new instance x_n , the new mean and scatter matrix can be computed as follows:

$$\mu_n = \mu_{n-1} + (x_n - \mu_{n-1})/n$$

$$S_n = S_{n-1} + (x_n - \mu_{n-1}) * (x_n - \mu_n)$$

In multidimensional spaces we have:

$$S_n = S_{n-1} + (x_n - \mu_{n-1}) * (x_n - \mu_n)^T$$

With some algebraic manipulations the updated S_n of Welford algorithm can be related only to μ_{n-1} as follows:

$$\begin{aligned} S_n &= S_{n-1} + \frac{n-1}{n} (x_n - \mu_{n-1}) * (x_n - \mu_{n-1})^T \\ &= S_{n-1} + yy^T \end{aligned}$$

where

$$y = \sqrt{\frac{n-1}{n}} (x_n - \mu_{n-1}) \quad (5)$$

and yy^T is a Hermitian matrix. Note that We will show the foreground instances have more contribution to the main eigenvector of S . Before that, it is necessary to prove some theorems and lemma.

In the following theorems, S_{n-1}, S_n and yy^T are demonstrated by A, A' and E , respectively. In the following theorem we will show that the differences of the first eigenvectors of A and A' have bounded from above, by a value related to E .

Theorem III.1. Let $A \in \mathbb{C}^{n \times n}$ is a Hermitian matrix, $A' = A + yy^*$ is rank one updated of A and $y \in \mathbb{C}^n$ is column

vector. If v and v' are the normalized eigenvectors of A and A' corresponding to their largest eigenvalues, then:

$$\|v - v'\| \leq \beta \|E\| \quad (6)$$

where $E = yy^*$ is a small perturbation of A and β is a value unrelated to E .

Proof. See Theorem A.1 in Appendix. \square

The left hand side of 6 is the differences of the main eigenvectors of A and $A + E$. It is bounded from above by $\beta \|E\|$, where $E = yy^T$ and $y = \sqrt{\frac{n-1}{n}}(x_n - \mu_{n-1})$. Hence the left hand side is related to the incoming instance x_n . We will show that the expected value of the eigenvector's variations, is more related to the foreground instances than others.

The expected value of the right hand side of 6 is:

$$\mathbb{E}[\beta \|E\|] = \beta \mathbb{E}[\|E\|] \quad (7)$$

In the next theorem, the relation of this expected value and the incoming instance is shown. For the sake of simplicity we drop the scalar coefficient $\sqrt{\frac{n-1}{n}}$ from y , then our perturbation matrix E will be:

$$E = (x_n - \mu_{n-1})(x_n - \mu_{n-1})^T$$

Lemma III.2. Let N_b, μ_b be the number and the mean of background instances until time $n - 1$; and N_f, μ_f be the mentioned parameters for the foreground's; and $N_b = N_f \approx (n - 1)/2$. If $E = (x_n - \mu_{n-1})(x_n - \mu_{n-1})^T$ and the new instance x_n belong to Background ($x_n \in B$), then

$$\mathbb{E}[\|E\|] \leq \mathbb{E}[\|x_n - \mu_b\|^2] + \mathbb{E}[\|x_n - \mu_f\|^2]$$

Proof. We know that the spectral norm of a Hermitian matrix is the absolute value of its largest eigenvalue [31]. Also, we know that the only non-zero eigenvalue of $E = uv^T$ is $v^T u$ (See Lemma A.4 in Appendix). E is a symmetric matrix, according to Lemma A.3 in Appendix we have:

$$\|E\|_2 = (x_n - \mu_{n-1})^T (x_n - \mu_{n-1})$$

With rewriting $x_n - \mu_{n-1}$ we have:

$$x_n - \mu_{n-1} = x_n - \frac{N_b \mu_b + N_f \mu_f}{n - 1}$$

Since $N_b = N_f = (n - 1)/2$, thus:

$$\begin{aligned} x_n - \mu_{n-1} &= x_n - \frac{\mu_b + \mu_f}{2} \\ &= \frac{(x_n - \mu_b) + (x_n - \mu_f)}{2} \end{aligned}$$

Let $A = (x_n - \mu_b)/2$ and $B = (x_n - \mu_f)/2$. Then

$$\begin{aligned} \|E\|_2 &= (A + B)^T (A + B) \\ &= \langle A + B, A + B \rangle \\ &= \|A\|^2 + \langle A, B \rangle + \langle B, A \rangle + \|B\|^2 \\ &\leq \|A\|^2 + 2|\langle A, B \rangle| + \|B\|^2 \\ &= \|x_n - \mu_b\|_2^2 + 2(x_n - \mu_b)^T (x_n - \mu_f) \\ &\quad + \|x_n - \mu_f\|_2^2 \end{aligned}$$

Thus:

$$\|E\|_2 \leq \|x_n - \mu_b\|_2^2 + \|x_n - \mu_f\|_2^2 + C_1 = \text{UB}$$

where $C_1 = 2(x_n - \mu_b)^T (x_n - \mu_f)$. The expected value of upper bound UB is given by

$$\begin{aligned} \mathbb{E}[\text{UB}] &= \mathbb{E}[\|x_n - \mu_b\|_2^2 + \|x_n - \mu_f\|_2^2 + C_1] \\ &= \mathbb{E}[\|x_n - \mu_b\|_2^2] + \mathbb{E}[\|x_n - \mu_f\|_2^2] + \mathbb{E}[C_1] \end{aligned} \quad (8)$$

Since $x_n \in B$, hence $\mathbb{E}[x_n] = \mu_b$, then:

$$\begin{aligned} \mathbb{E}[C_1] &= \mathbb{E}[2(x_n - \mu_b)^T (x_n - \mu_f)] \\ &= 2\mathbb{E}[x_n^T x_n - x_n^T \mu_b - x_n^T \mu_f + \mu_b^T \mu_f] \\ &= 2(\mathbb{E}[x_n^T x_n] - \mathbb{E}[x_n^T] \mu_b - \mathbb{E}[x_n^T] \mu_f + \mu_b^T \mu_f) \\ &= 2(\mu_b^T \mu_b - \mu_b^T \mu_b - \mu_b^T \mu_f + \mu_b^T \mu_f) = 0 \end{aligned}$$

Hence, we have:

$$\mathbb{E}(\|E\|) \leq \mathbb{E}[\|x_n - \mu_b\|^2] + \mathbb{E}[\|x_n - \mu_f\|^2] \quad \square$$

For the sake of simplicity, temporary, we will drop n from x_n , and x denotes the incoming frame, which may be belong to background (B) or foreground (F).

Lemma III.3. Suppose that $x = [x^1, \dots, x^j, \dots, x^m]^T \in B$ indicate an instance of background frames (B) over time. If $(\sigma_b^j)^2$ is the variance of the j^{th} component of x , then $\mathbb{E}[\|x - \mu_b\|^2] = \sum_{j=1}^m (\sigma_b^j)^2$.

Proof. Assume that $x, \mu_b \in \mathbb{R}^m$, then:

$$\begin{aligned} \|x - \mu_b\|^2 &= \sum_{j=1}^m (x^j - \mu_b^j)^2 \text{ follows that} \\ \mathbb{E}[\|x - \mu_b\|^2] &= \mathbb{E}[\sum_{j=1}^m (x^j - \mu_b^j)^2] \\ &= \sum_{j=1}^m \mathbb{E}[(x^j - \mu_b^j)^2] = \sum_{j=1}^m (\sigma_b^j)^2 \quad (x \in B) \end{aligned} \quad \square$$

If $x \in F$ (Indicating a foreground instance), with the same induction of the previous Lemma, we will have:

$$\mathbb{E}[\|x - \mu_f\|^2] = \sum_{j=1}^m (\sigma_f^j)^2 \quad (9)$$

According the assumption 2, we have:

$$(\sigma_b^j)^2 \ll (\sigma_f^j)^2, \quad \forall j$$

If the above summations $\sum_{j=1}^m (\sigma_b^j)^2, \sum_{j=1}^m (\sigma_f^j)^2$ demonstrated by Σ_b^2, Σ_f^2 , we have:

$$\Sigma_b^2 \ll \Sigma_f^2 \quad (10)$$

Here we investigated the expected value of the upper bound UB, where x belongs to background or foreground. At first, suppose $x \in B$, hence we have:

$$\mathbb{E}[x] = \mu_b$$

Proposition 1. *With notation as above, if $x \in B$, then*

$$\mathbb{E}[\|E\|] \leq \Sigma_b^2 + C$$

where C is a constant, unrelated to x

Proof.

$$\begin{aligned} \mathbb{E}(\|E\|) &\leq \mathbb{E}[\|x - \mu_b\|^2] + \mathbb{E}[\|x - \mu_f\|^2] \\ &\quad \text{(According to Lemma III.2)} \\ &= \Sigma_b^2 + \mathbb{E}[\|x - \mu_f\|^2] \quad \text{(According to Lemma III.3)} \end{aligned}$$

In fact,

$$\begin{aligned} \mathbb{E}[\|x - \mu_f\|^2] &= \mathbb{E}[x^T x - 2x^T \mu_f + \mu_f^T \mu_f] \\ &= \mathbb{E}[x^T x] - 2\mathbb{E}[x^T] \mu_f + \mu_f^2 \\ &= \mu_b^T \mu_b - 2\mu_b^T \mu_f + \mu_f^T \mu_f = C \end{aligned}$$

Thus,

$$\mathbb{E}[\|E\|] \leq \Sigma_b^2 + C$$

□

Remark 1. *Lemma III.2, III.3 and Proposition 1 were proved when $x \in B$. With similar induction it is clear that these are true when $x \in F$ (the new instance belongs to Foreground). Hence these Lemmas and Proposition are true for every instance (whether belongs to background or foreground). Note that for foreground instances Σ_b^2 should be replaced by Σ_f^2 , i.e.:*

$$\mathbb{E}[\|E\|] \leq \Sigma_f^2 + C$$

Theorem III.4. *Let $A \in \mathbb{C}^{n \times n}$ be a Hermitian matrix, $A' = A + yy^*$ be a rank one updated of A and $y \in \mathbb{C}^n$ be column vector constructed by the arrived instance x_n (eq. 5). Suppose v and v' be the normalized eigenvectors of A and A' corresponding to their largest eigenvalues, and $\theta_b(\theta_f)$ be the angle between v and v' , when the new instance belongs to background(foreground). If $\Sigma_b^2 \ll \Sigma_f^2$ then*

$$\mathbb{E}[\theta_b] \ll \mathbb{E}[\theta_f]$$

Proof. According to Theorem III.1, the upper bound of $\|v - v'\|$ is $\beta \|E\|$ and according to Proposition 1 and Remark 1, the expected value of the upper bound is:

$$\mathbb{E}[\theta_b] = \mathbb{E}[\|v - v'\|] \leq \beta(\Sigma_b^2 + C) \quad \text{if } x_n \in B \quad (11)$$

$$\mathbb{E}[\theta_f] = \mathbb{E}[\|v - v'\|] \leq \beta(\Sigma_f^2 + C) \quad \text{if } x_n \in F \quad (12)$$

For a specific signal $X = \{x_1, \dots, x_{n-1}\}$ the values β, C are unrelated to incoming instance x_n ; since $\Sigma_b^2 \ll \Sigma_f^2$, we have $\mathbb{E}[\theta_b] \ll \mathbb{E}[\theta_f]$. □

Corollary III.5. *Let $X = \{x_1, \dots, x_{n-1}\}$ be the previous instances of the signal, and $x_n \in B \cup F$ is the last incoming instance; and B, F denote the Background or the Foreground sets. Suppose that the variances of background instances be less than foregrounds. Then it is expected that the first principal component of X to be more affected when $x_n \in F$, than when $x_n \in B$.*

Proof. The first principal component of X is the normalized eigenvector v corresponding to the largest eigenvalue of scatter matrix $A = S_{n-1} = \sum_{k=1}^{n-1} (x_k - \mu)(x_k - \mu)^T$. By arriving the

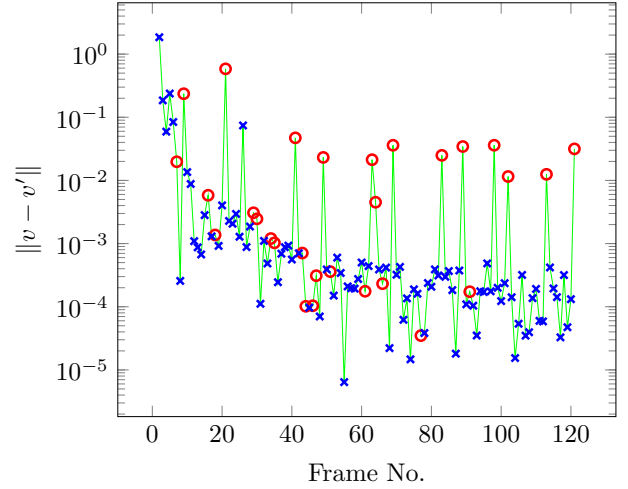


Fig. 9. Changes in the main eigenvector (i.e. the eigenvector belong to the largest eigenvalue) for every new frame added by calculating the norm of the difference between the old vector v and the new vector v' . The blue x demonstrate background frames and the red circles are for foreground frames. This shows that foreground frames are more influential than background frames in changing the main eigenvector.

new instance x_n , the new eigenvector v' is about the same for the new scatter matrix $A' = S_n$. A is a Hermitian matrix and A' is a rank one updated of A . So, if θ_b be the angle between v and v' when $x_n \in B$ and θ_f when $x_n \in F$, then according to Theorem III.4, the proof is straightforward. □

IV. EXPERIMENTAL RESULTS

The previous mathematical discussion showed the main idea of this paper: foreground frames have the most significant role in the direction of the main eigenvector. We saw this phenomenon in figure 5. The dominant PCA vector was influenced mostly by foreground frames. As a result the modeled background in figure 8 was superior to figure 7.

In Figure 9 we calculated and showed the norm differences of the main eigenvectors for every new frame added ($\|v - v'\|$). As can be clearly seen in this figure, the main eigenvector is more influenced by foreground frames than background ones. It is an evidence for Theorems III.4 and III.5. In average, eigenvector's variations due to foreground frames are greater than those related to backgrounds. Frames and their orders are as same as figure 5.

As another experiment, for the same block shown in Figure 3, we computed all 121 eigenvectors (121 frames resulted in 121 eigenvectors). Then for every frame, the projected image on the subspace of the first two eigenvectors is demonstrated in Figure 10. This figure shows how image frames are distributed in the 2D space defined by two consequence eigenvectors. As before, the red circles demonstrate foreground frames and blue crosses show background frames. Subfigures (a)–(e) show the subspaces corresponding to the following eigenvectors' pairs: (1,2), (25,26), (49,50), (73,74) and (97,98), respectively.

Let explain figure 10(a): left panel shows the first and second eigenvectors. As can be seen, the blue crosses that belong to background frames are mapped very closely while the red circles, demonstrated the foreground frames, are distributed in

this 2D space. This shows this subspace is indeed suitable for foreground objects and not for background region. For better visualization, the right panel shows some uniformly selected frames from the left panel points. If we divide the whole space to a 5×5 hypothetical grid, these 25 images are the closest projected images to the vertices of this grid. The corresponding points are marked by a green plus sign in the left panel (behind red and blue markers).

Similarly, we created a 2D space defined by some other eigenvectors and again mapped all frames into this 2D space as explained above. The result is shown in Figure 10(b)–(e). Figure (e) shows less significant components (97 and 98). In contrast to Figure 10(a), in the 2D space defined by these non-significant eigenvectors, all foreground frames are mapped very closely to each other while background frames are widely distributed. These figures show most significant eigenvectors are more suitable to model and analysis of different foreground objects while the space defined by least significant eigenvectors are more proper for background.

Figures 11 and 12 show the aforementioned experiments on two videos: *ShoppingMall* and *Traffic*. Both of them have more crowded than *Highway*. As the previous results in figure 10, the most important eigenvectors, illustrate the foreground space, and by increasing the component numbers – or least significant eigenvectors – the background frames (blue markers) are more distributed. In the last two videos, even in the least significant components, red markers (or foreground frames) are also spread out over the whole space. The reason is that these videos are taken from a very crowded place, and almost in all frames, a moving object was present in every block.

As can be seen, in all three figures, the subspace spanned by the weakest eigenvectors – subfigures (a) – the background instances (blue crosses) are compacted and not spread well. By increasing the principal component number, background instances are spread and foreground ones are compressed.

V. CONCLUSION

Eigenbackground [1] is a well-known method for background modeling. Where in this method the most significant eigenvectors is selected for background modeling. In this paper, this method was investigated and proved that the subspace produced by the most significant eigenvectors does not reflect the nature of the background. Theoretical aspects of this investigation were also confirmed by experimental results. This finding explain various artifacts reported by researchers on using Eigenbackground method.

On the other hand, least significant eigenvectors are considered less important in computer vision and image literature application as they are considered to be highly affected by noise and other distortions in the input images/videos. In most applications, this information is thrown away and treated as “garbage data”. However, this information can actually be useful for specific applications such as background modeling. In fact, as shown in this paper, the least significant eigenvectors perform much better than most significant eigenvectors in modeling background and extracting foreground objects in video frames.

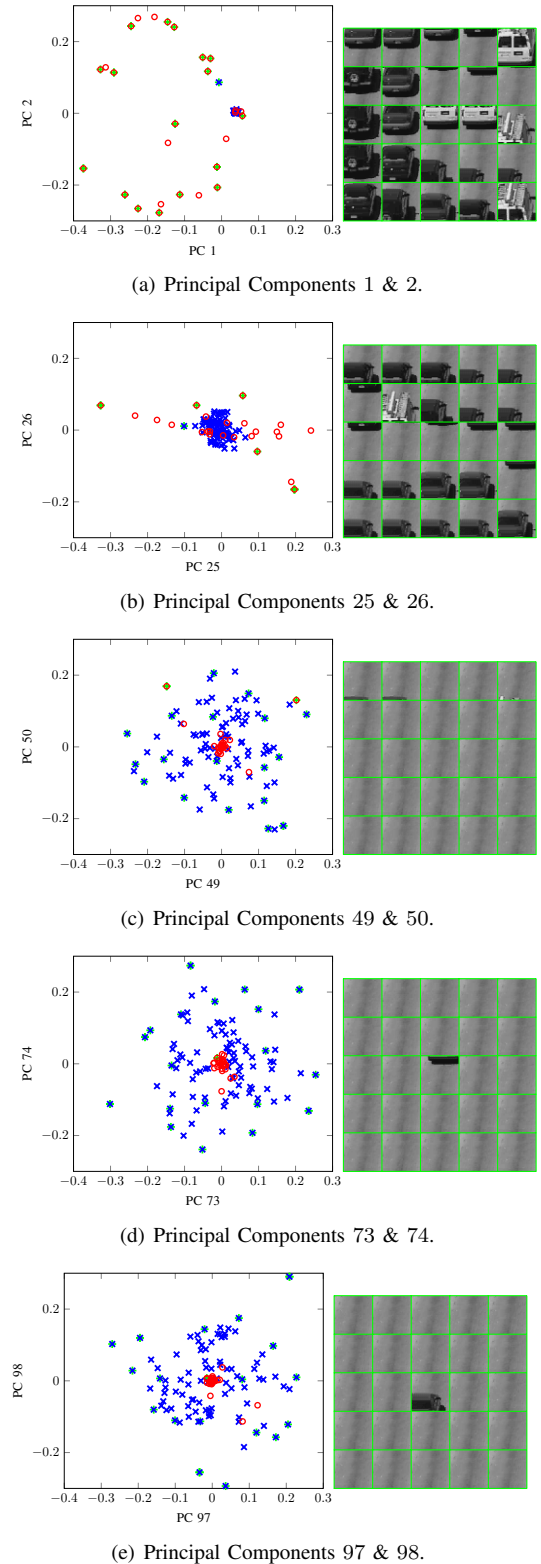
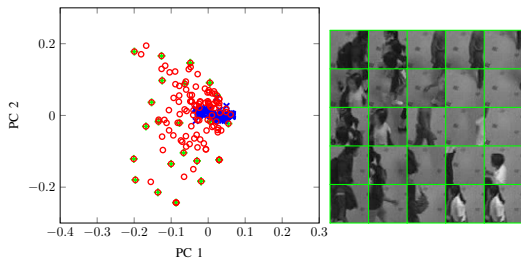
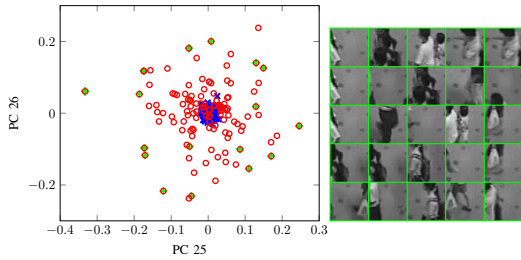


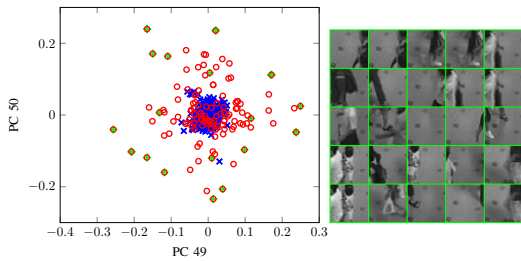
Fig. 10. Some demonstration for the effect of different principal components subspaces for video: *Highway*. (Left panel:) the principal components’ subspace of the video. The blue crosses/red circles, show background/foreground images. The green plus points are the closest projected images to the vertices of a unified grid, defined by the marginal of the principal components. (Right panel:) The images corresponding to the green plus points. Foreground images are well distributed in subspaces related to strongest eigenvectors (first eigenvectors); in contrast background frames are well propagated in subspaces corresponding to the weakest eigenvectors.



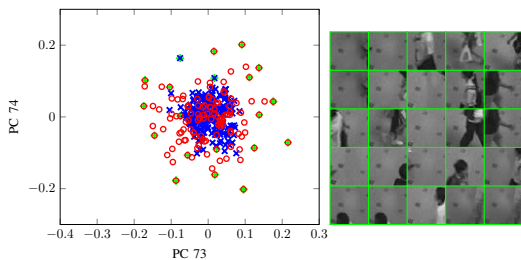
(a) Principal Components 1 & 2.



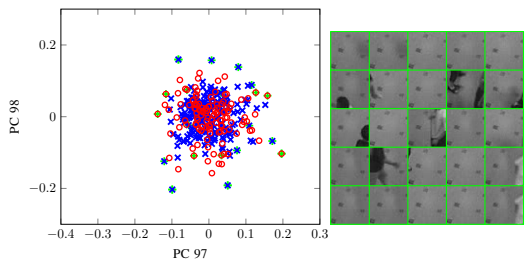
(b) Principal Components 25 & 26.



(c) Principal Components 49 & 50.

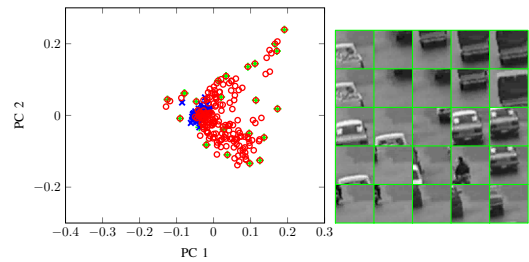


(d) Principal Components 73 & 74.

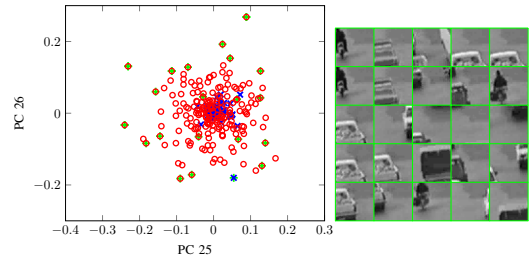


(e) Principal Components 97 & 98.

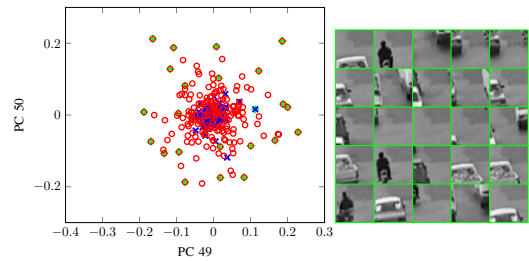
Fig. 11. Some demonstration for the effect of different principal components subspaces for video: *ShoppingMall*. (Left panel:) the principal components' subspace of the video. The blue crosses/red circles, show background/foreground images. The green plus points are the closest projected images to the vertices of a unified grid, defined by the marginal of the principal components. (Right panel:) The images corresponding to the green plus points. Foreground images are well distributed in subspaces related to strongest eigenvectors (first eigenvectors); in contrast background frames are well propagated in subspaces corresponding to the weakest eigenvectors.



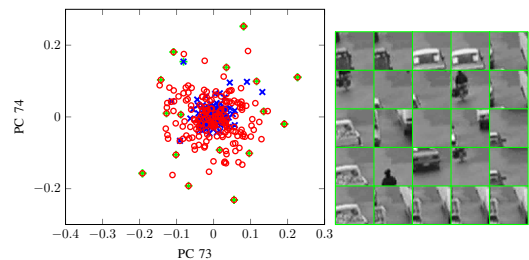
(a) Principal Components 1 & 2.



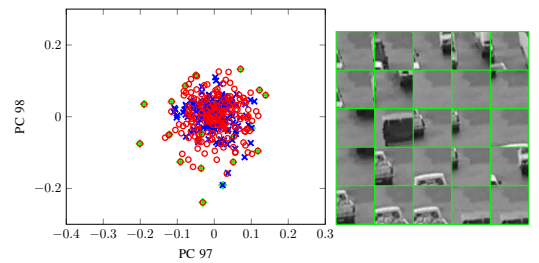
(b) Principal Components 25 & 26.



(c) Principal Components 49 & 50.



(d) Principal Components 73 & 74.



(e) Principal Components 97 & 98.

Fig. 12. Some demonstration for the effect of different principal components subspaces for video: *Traffic*. (Left panel:) the principal components' subspace of the video. The blue crosses/red circles, show background/foreground images. The green plus points are the closest projected images to the vertices of a unified grid, defined by the marginal of the principal components. (Right panel:) The images corresponding to the green plus points. Foreground images are well distributed in subspaces related to strongest eigenvectors (first eigenvectors); in contrast background frames are well propagated in subspaces corresponding to the weakest eigenvectors.

REFERENCES

- [1] N. M. Oliver, B. Rosario, and A. P. Pentland, "A Bayesian computer vision system for modeling human interactions," *IEEE Transactions on Pattern Analysis and Machine Intelligence*, vol. 22, pp. 831–843, Aug. 2000.
- [2] F. De La Torre and M. J. Black, "Robust principal component analysis for computer vision," in *Computer Vision, 2001. ICCV 2001. Proceedings. Eighth IEEE International Conference on*, vol. 1, pp. 362–369 vol.1, IEEE, 2001.
- [3] D. Skočaj and A. Leonardis, "Incremental and robust learning of subspace representations," *Image and Vision Computing*, vol. 26, no. 1, pp. 27–38, 2008.
- [4] P. Dickinson, A. Hunter, and K. Appiah, "A spatially distributed model for foreground segmentation," *Image and Vision Computing*, vol. 27, no. 9, pp. 1326–1335, 2009.
- [5] Y. Yuan, Y. Pang, J. Pan, and X. Li, "Scene segmentation based on ipca for visual surveillance," *Neurocomputing*, vol. 72, no. 10–12, pp. 2450–2454, 2009. cited By 23.
- [6] M. Casares, S. Velipasalar, and A. Pinto, "Light-weight salient foreground detection for embedded smart cameras," *Computer Vision and Image Understanding*, vol. 114, no. 11, pp. 1223–1237, 2010. cited By 20.
- [7] Y. Dong and G. Desouza, "Adaptive learning of multi-subspace for foreground detection under illumination changes," *Computer Vision and Image Understanding*, vol. 115, no. 1, pp. 31–49, 2011. cited By 15.
- [8] K. Tzevanidis and A. Argyros, "Unsupervised learning of background modeling parameters in multicamera systems," *Computer Vision and Image Understanding*, vol. 115, no. 1, pp. 105–116, 2011. cited By 5.
- [9] C. Guyon, T. Bouwmans, and E.-H. Zahzah, "Robust Principal Component Analysis for Background Subtraction: Systematic Evaluation and Comparative Analysis," in *Principal Component Analysis, Book 1*, pp. 223–238, INTECH, Mar. 2012.
- [10] L. Vosters, C. Shan, and T. Gritti, "Real-time robust background subtraction under rapidly changing illumination conditions," *Image and Vision Computing*, vol. 30, no. 12, pp. 1004–1015, 2012.
- [11] M. G. Krishna, V. M. Aradhya, M. Ravishankar, and D. R. Babu, "Lopp: Locality preserving projections for moving object detection," *Procedia Technology*, vol. 4, pp. 624 – 628, 2012. 2nd International Conference on Computer, Communication, Control and Information Technology(C3IT-2012) on February 25 - 26, 2012.
- [12] Y. Zhao, H. Gong, Y. Jia, and S.-C. Zhu, "Background modeling by subspace learning on spatio-temporal patches," *Pattern Recognition Letters*, vol. 33, no. 9, pp. 1134–1147, 2012. cited By 9.
- [13] B. Yeo, W. Lim, and H. Lim, "Scalable-width temporal edge detection for recursive background recovery in adaptive background modeling," *Applied Soft Computing Journal*, vol. 13, no. 4, pp. 1583–1591, 2013.
- [14] R. Seger, M. Wanderley, and A. Koerich, "Automatic detection of musicians' ancillary gestures based on video analysis," *Expert Systems with Applications*, vol. 41, no. 4 PART 2, pp. 2098–2106, 2014.
- [15] C. Spampinato, S. Palazzo, and I. Kavasidis, "A texton-based kernel density estimation approach for background modeling under extreme conditions," *Computer Vision and Image Understanding*, vol. 122, pp. 74–83, 2014.
- [16] T. Bouwmans, "Traditional and recent approaches in background modeling for foreground detection: An overview," *Computer Science Review*, vol. 11–12, pp. 31 – 66, 2014.
- [17] S. Varadarajan, P. Miller, and H. Zhou, "Region-based mixture of gaussians modelling for foreground detection in dynamic scenes," *Pattern Recognition*, vol. 48, no. 11, pp. 3488–3503, 2015.
- [18] M. Shakeri and H. Zhang, "COROLA: A sequential solution to moving object detection using low-rank approximation," *CoRR*, vol. abs/1505.03566, 2015.
- [19] J. Dou, J. Li, Q. Qin, and Z. Tu, "Moving object detection based on incremental learning low rank representation and spatial constraint," *Neurocomputing*, vol. 168, pp. 382–400, 2015.
- [20] Z. Xu, P. Shi, and I. Y. H. Gu, "An eigenbackground subtraction method using recursive error compensation," in *PCM (Y. Zhuang, S. Yang, Y. Rui, and Q. He, eds.)*, vol. 4261 of *Lecture Notes in Computer Science*, pp. 779–787, Springer, 2006.
- [21] W. Chen, Y. Tian, Y. Wang, and T. Huang, "Fixed-point gaussian mixture model for analysis-friendly surveillance video coding," *Computer Vision and Image Understanding*, vol. 142, pp. 65–79, 2016.
- [22] M. Wan, G. Gu, W. Qian, K. Ren, Q. Chen, H. Zhang, and X. Maldague, "Total variation regularization term-based low-rank and sparse matrix representation model for infrared moving target tracking," *Remote Sensing*, vol. 10, no. 4, p. 510, 2018.
- [23] S. Banu and N. Maheswari, "Background modelling using a q-tree based foreground segmentation," *Scalable Computing: Practice and Experience*, vol. 21, pp. 17–31, 03 2020.
- [24] A. Djerida, Z. Zhao, and J. Zhao, "Background subtraction in dynamic scenes using the dynamic principal component analysis," *IET Image Processing*, vol. 14, no. 2, pp. 245–255, 2020.
- [25] M. Amintoosi, F. Farbiz, and M. Fathy, "A QR Decomposition based mixture model algorithm for background modeling," in *ICICS2007, Sixth International InProceedings on Information, Communication and Signal Processing*, (Singapore), pp. 1–5, December 2007.
- [26] M. Amintoosi, F. Farbiz, M. Fathy, M. Analoui, and N. Mozayani, "QR decomposition-based algorithm for background subtraction.," in *ICASSP (1)*, pp. 1093–1096, IEEE, 2007.
- [27] C. Stauffer and W. E. L. Grimson, "Adaptive background mixture models for real-time tracking," in *Computer Vision and Pattern Recognition, 1999. IEEE Computer Society Conference on.*, vol. 2, (Los Alamitos, CA, USA), pp. 246–252 Vol. 2, IEEE, Aug. 1999.
- [28] M. Setnes and R. Babuska, "Rule base reduction: Some comments on the use of orthogonal transforms," *Trans. Sys. Man Cyber Part C*, vol. 31, p. 199–206, May 2001.
- [29] R. O. Duda, P. E. Hart, and D. G. Stork, *Pattern Classification (2Nd Edition)*. Wiley-Interscience, 2000.
- [30] B. P. Welford, "Note on a method for calculating corrected sums of squares and products," *Technometrics*, vol. 4, no. 3, pp. 419–420, 1962.
- [31] G. W. Stewart, *Introduction to matrix computations*, vol. Computer science and applied mathematics. Academic Press, 1973.
- [32] I. C. F. Ipsen and B. Nadler, "Refined perturbation bounds for eigenvalues of hermitian and non-hermitian matrices," *SIAM J. Matrix Analysis Applications*, vol. 31, no. 1, pp. 40–53, 2009.
- [33] V. Zemlys. <http://math.stackexchange.com/questions/9302/norm-of-a-symmetric-matrix>, 2011.

APPENDIX

Theorem A.1. *Suppose that $A \in \mathbb{C}^{n \times n}$ is a Hermitian matrix, $A' = A + yy^*$ is rank one updated of A and $y \in \mathbb{C}^n$ is column vector. If v and v' are the normalized eigenvectors of A and A' corresponding to their largest eigenvalues, then:*

$$\|v - v'\| \leq \beta \|E\| \quad (13)$$

where $E = yy^*$ is a small perturbation of A and β is a value unrelated to E .

Proof. Suppose that λ and λ' are the largest eigenvalues of A and A' . By definition of eigenvector we have

$$\begin{aligned} Av &= \lambda v \\ A'v' &= \lambda'v' \end{aligned}$$

According to Proposition 2 there is an $\epsilon > 0$ such that $\lambda + \epsilon = \lambda'$. Hence:

$$\begin{aligned} (A + E)v' - Av &= \lambda'v' - \lambda v \\ &= (\lambda + \epsilon)v' - \lambda v \end{aligned} \quad (14)$$

Thus:

$$\begin{aligned}
A(v' - v) + Ev' &= \lambda v' + \epsilon v' - \lambda v \\
&\Rightarrow \\
(A - \lambda I)(v' - v) &= (\epsilon I - E)v' \\
&\Rightarrow \\
v' - v &= (A - \lambda I)^{-1}(\epsilon I - E)v' \\
&\Rightarrow \\
\|v' - v\| &= \|(A - \lambda I)^{-1}(\epsilon I - E)v'\| \\
&\leq \underbrace{\|(A - \lambda I)^{-1}\|}_{\alpha} \|(\epsilon I - E)v'\| \underbrace{\|v'\|}_1 \\
&= \alpha \|(\epsilon I - E)v'\| \\
&\leq \alpha (\|\epsilon I\| + \alpha \|-E\|) \\
&\quad \text{(Triangle Inequality)} \\
&= \alpha (\epsilon + \|E\|) \\
&\leq \alpha (\|E\| + \|E\|) \\
&\quad \text{(According to Proposition 2: } \epsilon \leq \|E\|) \\
&= \beta \|E\| \tag{15}
\end{aligned}$$

where $\beta = 2\alpha$ \square

Lemma A.2. For a given Hermitian matrix $A \in \mathbb{C}^{n \times n}$ and a column vector $y \in \mathbb{C}^n$, we have:

$$\lambda_{max}(A) \leq \lambda_{max}(A + yy^*) \leq \lambda_{max}(A) + \|y\|^2$$

Proof. See [32]. \square

Lemma A.3. The norm of a symmetric matrix is maximum absolute value of its eigenvalue.

Proof. We have

$$\|A\|_2 = \max_{\|x\|=1} \|Ax\|$$

where $\|\cdot\|$ denotes the ordinary Euclidean norm. This is a constrained optimization problem with Lagrange function:

$$L(x, \lambda) = \|Ax\|^2 - \lambda(\|x\|^2 - 1) = x^T A^2 x - \lambda(x^T x - 1)$$

Taking squares makes the following step easier. Taking derivative with respect to x and equating it to zero we get

$$A^2 x - \lambda x = 0$$

the solution for this problem is the eigenvector of A^2 . Since A^2 is symmetric, all its eigenvalues are real. So $x^T A^2 x$ will achieve maximum on set $\|x\|^2 = 1$ with maximal eigenvalue of A^2 . Now since A is symmetric it admits representation

$$A = Q\Lambda Q^T$$

with Q the orthogonal matrix and Λ diagonal with eigenvalues in diagonals. For A^2 we get

$$A^2 = Q\Lambda^2 Q^T$$

so the eigenvalues of A^2 are squares of eigenvalues of A . The norm $\|A\|_2$ is the square root taken from maximum $x^T A^2 x$ on $x^T x = 1$, which will be the square root of maximal eigenvalue of A^2 which is the maximal absolute eigenvalue of A [33]. \square

Lemma A.4. Suppose $A = uv^T$ where u and v are non-zero column vectors in \mathbb{R}^n , $n \geq 3$. Then $\lambda = 0$ and $\lambda = v^T u$ are the only eigenvalues of A .

Proof. $\lambda = 0$ is an eigenvalue of A since A is not of full rank. $\lambda = v^T u$ is also an eigenvalue of A since

$$Au = (uv^T)u = u(v^T u) = (v^T u)u.$$

We assume $v \neq 0$. The orthogonal complement of the linear subspace generated by v (i.e. the set of all vectors orthogonal to v) is therefore $(n-1)$ -dimensional. Let $\phi_1, \dots, \phi_{n-1}$ be a basis for this space. Then they are linearly independent and $uv^T \phi_i = (v \cdot \phi_i)u = 0$. Thus the eigenvalue 0 has multiplicity $n-1$, and there are no other eigenvalues besides it and $v \cdot u$. \square

Proposition 2. In the previous lemmas (A.2, A.3 and A.4), assume that $E = yy^*$, then there exists an $0 \leq \epsilon \leq \|E\|$ such that:

$$\begin{aligned}
\lambda_{max}(A) + \epsilon &= \lambda_{max}(A + yy^*) \leq \lambda_{max}(A) + \|y\|^2 \\
&= \lambda_{max}(A) + \|E\|
\end{aligned}$$



Mahmood Amintoosi received his Ph.D. degree in 2011 from Iran University of Science and Technology, Tehran, Iran in the area of artificial intelligence. He is now assistant professor at faculty of Mathematics and Computer Science, Hakim Sabzevari University, Iran. His research interests include machine learning, computer vision, deep learning and combinatorial optimization. He was a member of the ACM and IEEE. He has published more than 60 peer reviewed papers.



Dr. Farzam Farbiz (M'02–SM'09) received his Ph.D. in 1999 from Amirkabir University of Technology, Tehran, Iran in the area of computational intelligence. He has extensive background in artificial intelligence and its applications in both academia (as an adjunct associate professor at NUS) and industry (startup founder, collaborating with industry partners such as Rolls Royce and Nestle) on different AI applications such as AI for games, AI for e-commerce, and AI for manufacturing. He is currently a senior scientist with the Department of

Computing & Intelligence, Institute of High Performance Computing (IHPC), Agency for Science, Technology, and Research (A*STAR), Singapore. His research interest in on using physics-based AI to improve the performance of current machine learning models, and how this new model can be benefited by the society.